Determination of the pK_a Values for the Mitomycin C Redox Couple by Titration, pH Rate Profiles, and Nernst–Clark Fits. Studies of Methanol Elimination, Carbocation Formation, and the Carbocation/Quinone Methide Equilibrium

Romesh C. Boruah and Edward B. Skibo*

Department of Chemistry and Biochemistry, Arizona State University, Tempe, Arizona 85287-1604

Received October 7, 1994 (Revised Manuscript Received January 25, 1995[⊗])

This report provides the results of a study of the mitomycin C (MMC) redox couple pK_a values employing spectrophotometric titration, pH rate profiles, and Nernst–Clark plots. Oxidized mitomycin C (MMC_{ox}) has three acid dissociations: pK_{a1} = −1.2 for the protonated quinone, pK_{a2} = 2.7 for the protonated indoline nitrogen, and pK_{a3} = 7.6 for the protonated aziridino nitrogen. Two-electron reduction to MMC_{red} results in a shift to higher pK_a values: pK_{a1} = 1.4 for the protonated 7-amino group, pK_{a2} = 5.1 to 6.1 for the protonated indoline nitrogen, and pK_{a3} = 9.1 for the protonated aziridino nitrogen. These pK_a values were successfully integrated into previous mechanistic studies. The general conclusions are that indoline nitrogen protonation prevents methanol elimination, that methanol elimination from MMC_{ox} and MMC_{red} are both specific acid catalyzed, and that there is a 100000-fold increase in the second-order rate constant for specific acid-catalyzed elimination of methanol upon reduction of MMC_{ox} to MMC_{red}. Finally, the formation and fate of the mitosene hydroquinone carbocation was studied in a mitosene model bearing an acetate leaving group. The carbocation species undergoes acid dissociation to the quinone methide (pK_a = 7.1) resulting in a pH dependence for product formation. Below pH 7.1 the carbocation species traps water and above this pH the quinone methide species traps both water and a proton.

Introduction

Mitomycin C is an antitumor antibiotic that is activated as an alkylating agent by reduction to the hydroquinone derivative.[1] Reduction is followed by elimination of methanol to afford the aromatized indole (aziridinomitosene hydroquinone) derivative, which is converted to an alkylating quinone methide species by aziridino ring opening (Scheme 1).[2] The importance of mitomycin C as an antitumor agent has prompted detailed studies of the mechanism of reductive alkylation of DNA.[3] An important requirement for a mechanistic understanding of mitomycin C is a knowledge of all the relevant pK_a values for both the oxidized (MMC_{ox}) and two-electron reduced (MMC_{red}) species. Thus far, only a pK_a in the range of 2.7 to 3 for MMC_{ox}[4–6] and a pK_a of 5.1[7] for MMC_{red} have been determined. These pK_a values have been assigned to acid dissociation from the protonated aziridino nitrogen of MMC_{ox} and MMC_{red}, respectively. Queries posed at the outset of the present study dealt with the identity of the other pK_a values of the MMC redox couple as well as how these pK_a values relate to previous mechanistic studies.

Scheme 1

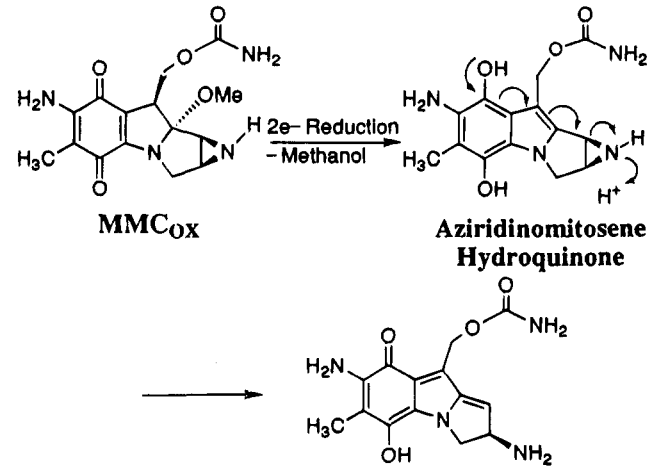

Provided in this report are the results of a study of the MMC pK_a values employing spectrophotometric titration, pH rate profiles, and Nernst–Clark plots.

The pK_a values thus determined are summarized in Scheme 2 for successive acid dissociation from triprotonated MMC species. The pK_a in the range of 2.7 to 3 is assigned to the protonated indoline nitrogen of MMC_{ox} rather than to the N-protonated aziridino group, which

[⊗] Abstract published in *Advance ACS Abstracts,* March 15, 1995.

(1) For reviews, see: (a) Remers, W. A. *The Chemistry of Antitumor Antibiotics*; Wiley: New York, 1979; Vol. I, pp 221–276. (b) Fisher, J. F.; Aristoff, P. A. *Prog. Drug Res.* **1988**, *32*, 411–498. (c) Franck, R. W.; Tomasz, M. In *The Chemistry of Antitumor Agents*; Wilman, D. E. V., Ed.; Blackie and Sons, Ltd.: Glasgow, Scotland, 1990; pp 379–394.

(2) Moore, H. W.; Czerniak, R. *Med. Res. Rev.* **1981**, *1*, 249–280.

(3) (a) Tomasz, M.; Lipman, R. *Biochemistry* **1981**, *20*, 5056–5061. (b) Tomasz, M.; Lipman, R.; Showdary, D.; Pawlak, J.; Verdine, G. L.; Nakanishi, K. *Science* **1987**, *235*, 1204–1208. (c) Tomasz, M.; Lipman, R.; McGuinness, B. F.; Nakanishi, K. *J. Am. Chem. Soc.* **1988**, *110*, 5892–5896. (d) Hopkins, P. B; Millard, J. T.;.Woo, J.; Weidner, M. F.; Kirchner, J. J.; Sigurdsson, S. T.; Raucher, S. *Tetrahedron* **1991**, *47*, 2475–2489. (e) For a recent monograph, see: *Bioreductive Activation, DNA Interaction, and Antitumor Activity of Mitosene Compounds*; Malliepaard, M., Ed.; Offsetdrukkerij Ridderprint B. V: Ridderkerk, 1994.

(4) Stevens, C. L.; Taylor, K. G.; Munk, M. E.; Marshall, W. S.; Noll, K.; Shah, G. D.; Shah, L. G.; Uzu, K. *J. Med. Chem.* **1964**, *8*, 1–10.

(5) McClelland, R. A.; Lam, K. *J. Am. Chem. Soc.* **1985**, *107*, 5182–5186.

(6) Similar pK_a values were also measured for mitomycins A and B: Beijnen, J. H.; van der Houwen, O. A. G. J.; Rosing, H.; Underberg, W. J. M. *Chem. Pharm. Bull.* **1986**, *34*, 2900–2913. See also: Beijmen, J. H.; van der Heuwen, O. A. G. J.; Paaij, J. D. F.; Paalman, A. C. A.; Underberg, W. J. M. *Int. J. Pharm.* **1988**, *45*, 189–196.

(7) Hoey, B. M.; Butler, J.; Swallow, A. J. *Biochemistry* **1988**, *27*, 2608–2614.

0022-3263/95/1960-2232$09.00/0

Scheme 2

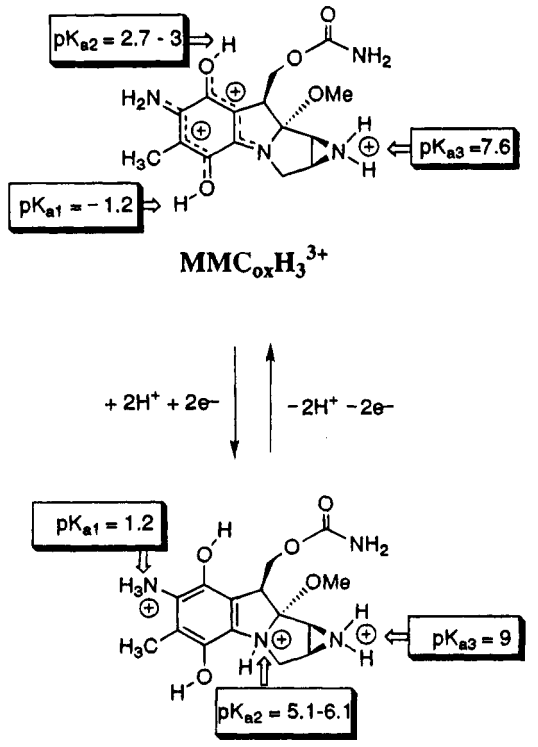

is now assigned a pK_a value more typical of an amine (pK_{a3} = 7.6). Two-electron reduction of MMC_{ox} affords MMC_{red}, which has all pK_a values shifted to higher values. The pK_a of 5.1 is assigned to acid dissociation from the protonated indoline nitrogen of MCC_{red}. Previous mechanistic studies are interpreted in terms of the new pK_a assignments.

Also provided are the results of a mechanistic study of carbocation formation by mitosene hydroquinone bearing an acetate bearing group. The carbocation intermediate loses a proton (p$K_a \approx 7.1$) to afford a quinone methide species capable of trapping protons and nucleophiles.

Results and Discussion

Determination of pK_{a1} and pK_{a2} for MMC_{ox}. Evidence that there are two acid dissociations present was obtained by following the rate of MMC_{ox} hydrolysis at 360 nm from pH −2 to 5. The disappearance of MMC_{ox} was first order over the entire pH range and independent of buffer at high acidity values. Shown in Figure 1 is a plot of log k_{obsd} vs pH obtained from these hydrolysis studies. The data in Figure 1 were fit to the two pK_a rate law shown in eq 1

$$k_{obsd} = \frac{k'a_H^2 + k''a_H K_{a1}}{a_H^2 + K_{a1}a_H + K_{a1}K_{a2}} \quad (1)$$

where k', k'', K_{a1}, and K_{a2} are constants in the generic process shown in eq 2, which does not address the mechanistic details of mitomycin C decomposition. The solid line in Figure 1 was computer generated from eq 1 where $k' = 0.26\ s^{-1}$, $k'' = 2.99 \times 10^{-3}\ s^{-1}$, p$K_{a1} = -1.28$, p$K_{a2} = 2.72$.

The value of pK_{a2} (2.72) is approximately the same as the value previously determined by titration[4] and by pH rate studies.[5] The value of pK_{a1} was not apparent in

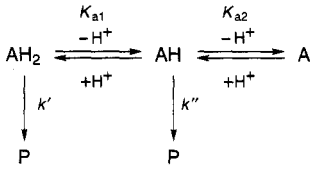

(2)

previous studies since the pH range of the kinetic studies did not extend below pH 1.[5] Evidence that this pK_a value is a thermodynamic rather than a kinetic quantity (i.e. a mixture of constants[8]) was obtained from a spectrophotometric (360 nm) titration of MMC_{ox} at high acidity. The value of pK_a thus obtained was -0.78 ± 0.07, which is nearly the same as the kinetically determined value.

The identity of the protons associated with these pK_a values were assigned on the basis of precedents. The values of p$K_a = -1.2$ and 2.7 are typical of acid dissociation from a protonated aminoquinone rather than from a protonated aziridino nitrogen.[9] The pK_a for the protonated aziridino nitrogen of MMC_{ox} was determined to be 7.60 on the basis of a Nernst–Clark fit (*vide infra*). Examples of pK_a values for acid dissociation from the protonated aminoquinones are shown in Scheme 3. The acid dissociation for $\mathbf{1}_{ox}\mathbf{H}^+$ and $\mathbf{3}_{ox}\mathbf{H}^+$ were determined spectrophotometrically at 317 and 525 nm, respectively, as part of the present study. The acid dissociation from $\mathbf{2}_{ox}\mathbf{H}^+$ was previously determined in this laboratory.[10] Quinone carbonyl protonation to afford a delocalized cation is considered for $\mathbf{1}_{ox}\mathbf{H}^+$ and $\mathbf{3}_{ox}\mathbf{H}^+$. Other examples of p$K_a$ values for protonated nitrogens substituted on a benzoquinone (hydroquinone) ring include: −2 (2.1),[11] 1.59 (4.7),[11] 1.15 (4.58),[10] 1.54 (6.02),[12] −0.05 (2.80).[13] From the above examples, it is apparent that the MMC_{ox} pK_a value of 2.7 is at the high end of aminoquinone pK_a values. Internal hydrogen bonding, as shown in the inset of Scheme 3, would stabilize the protonated quinone resulting in an increase in pK_a value above the examples cited. The second protonation of the MMC_{ox} quinone ring (p$K_a = -1.2$) to afford a dication species is expected to have a negative pK_a value.

The hydrolytic chemistry of MMC_{ox} will now be interpreted in terms of the pK_a assignments above. The solvolysis of MMC_{ox} in acid is known to involve the elimination of methanol and opening of aziridino ring and eventually replacement of the 7-amino group with a hydroxyl group.[4,14,15] McClelland and Lam[5] reported that the initial step is the acid-catalyzed elimination of methanol from MMC_{ox}. Their mechanistic study focused on the high pH plateau (pH > 1) in Figure 1 and considered that the pK_a of 2.7 is due to acid dissociation from the protonated aziridino nitrogen. It was postulated that the protonated aziridino species could not eliminate methanol since a doubly positive charged species would form (the iminium ion intermediate in Scheme 4). Therefore, the elimination of methanol must occur from neutral MMC_{ox} by specific acid and general acid-catalyzed processes. Scheme 4 has the essential features of the

(8) Bruice, T. C.; Schmir, G. L. *J. Am. Chem. Soc.* **1959**, *81*, 4552–4556.
(9) Dermer, O. C.; Ham, G. E. *Ethyleneimines and Other Aziridines*; Academic Press: New York, 1969; p 108.
(10) Skibo, E. B.; Gilchrist, J. H.; Lee, C.-H. *J. Org. Chem.* **1986**, *51*, 4784–4792.
(11) Lemus, R. H.; Lee, C. -H.; Skibo, E. B. *J. Org. Chem.* **1989**, *54*, 3611–3618.
(12) Islam, I.; Skibo, E. B. *J. Org. Chem.* **1990**, *55*, 3195–3205.
(13) Lemus, R. H.; Skibo, E. B. *J. Org. Chem.* **1988**, *53*, 6099–6105.
(14) Taylor, W. G.; Remers, W. A. *Tetrahedron. Lett.* **1974**, *39*, 3483–3486.
(15) Taylor, W. G.; Remers, W. A. *J. Med. Chem.* **1975**, *18*, 307–311.

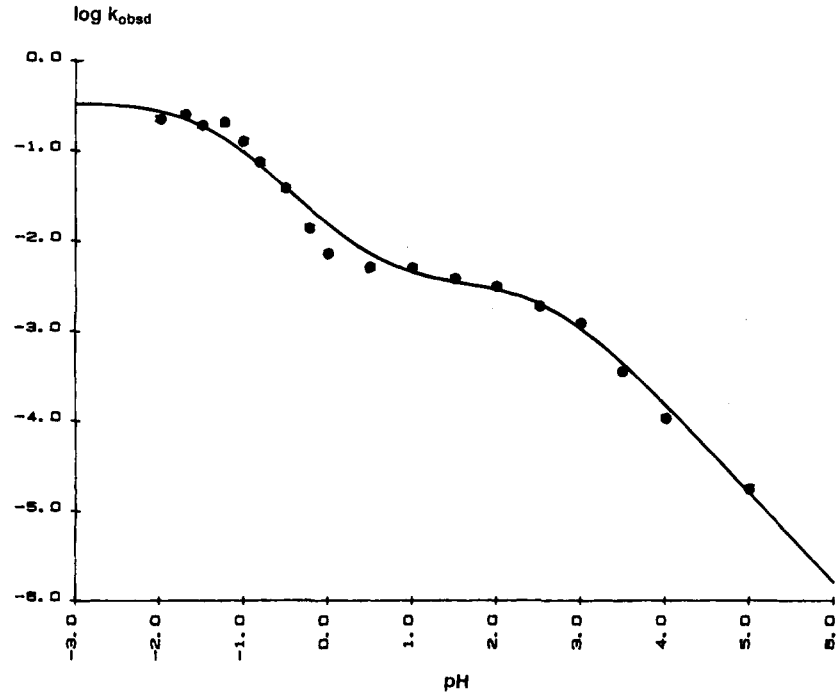

Figure 1. Plot of log k_{obsd} vs pH for the hydrolysis of MMC_{ox} in aerobic buffer (μ = 1.0, KCl) at 30.0 ± 0.2 °C.

Scheme 3

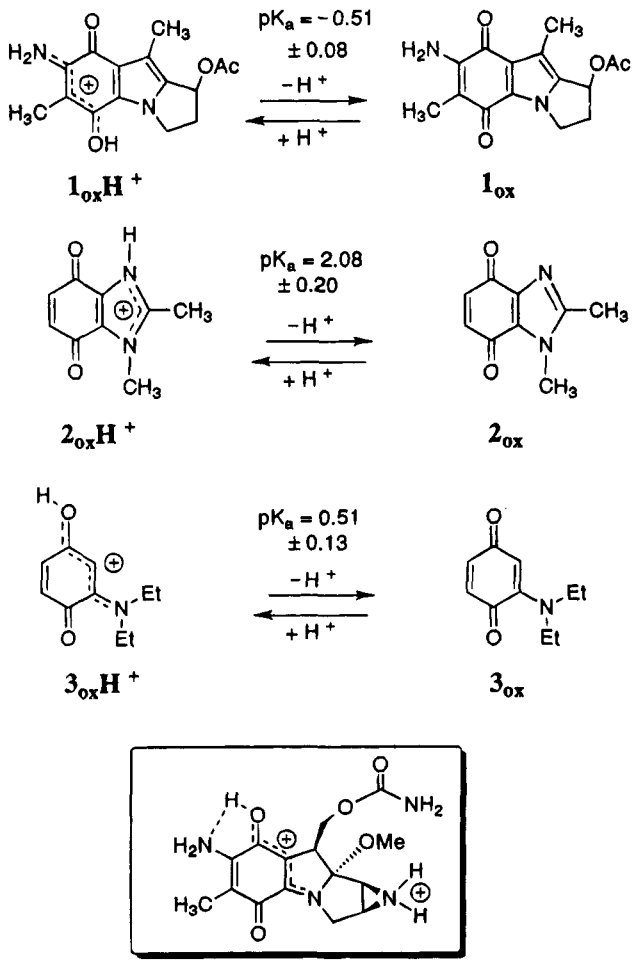

McClelland and Lam mechanism, except that acid-catalyzed methanol elimination occurs from $MMC_{ox}H^+$ rather than from MMC_{ox}.

According to Scheme 4, $MMC_{ox}H_2^{2+}$ cannot eliminate methanol since the indoline nitrogen bears a partial positive charge and the lone pair cannot be utilized to eliminate methanol. Thus, acid-catalyzed elimination of methanol must occur from $MMC_{ox}H^+$ to afford the iminium ion intermediate (see inset of Scheme 4). The formation of this doubly positive charged intermediate would be electrostatically unfavorable as a result of inductive (through-bond) effects, which should merely slow the methanol elimination rather than prevent it from occurring, see studies of Holmquist and Bruice.[16] In contrast, the mechanism wherein $MMC_{ox}H^+$ has a pK_a of 2.7 requires that such an elimination not occur at all.

Interpretation of the pH rate data in Figure 1 in terms of the mechanism in Scheme 4 provides eq 3:

$$k_{obsd} = \frac{k_1 a_H^{\,2} + k_2 a_H K_{a1} K_{a2}}{a_H^{\,2} + K_{a1} a_H + K_{a1} K_{a2}} \qquad (3)$$

where $k_1 = 0.26\ s^{-1}$ and $k_2 = 1.56\ M^{-1}\ s^{-1}$ and the pK_a values are the same as determined from eq 1. It should be pointed out that eqs 1 and 3 are kinetically identical, but the latter equation considers the mechanistic details of MMC_{ox} decomposition. The value of k_2, obtained at 30 °C, is nearly the same as the value of 1.2 $M^{-1}\ s^{-1}$ previously obtained at 25 °C.[5]

Determination of pK_{a1}, and pK_{a3} for MMC_{red} and pK_{a3} for MMC_{ox}, Nernst–Clark Plots. Hoey et al.[7] have determined that MMC_{red} possesses a pK_a of 5.1, which they have attributed to acid dissociation from the protonated aziridino nitrogen. This pK_a value (assigned pK_{a2} for MMC_{red}) along with pK_{a1} and pK_{a2} for MMC_{ox} were substituted into the Nernst–Clark equation[17,18] and the remaining pK_a values for the MMC couple solved for by fitting this equation to E_m vs pH data. The methodology involved is discussed below.

In order to illustrate the use of the Nernst–Clark equation in determining a pK_a value, the mitosene redox couple $\mathbf{1_{ox}/1_{red}}$ is discussed in conjunction with Figure 2.

(16) This reference discusses the degree of electrostatic stabilization and destabilization during ester hydrolysis: Holmquist B.; Bruice, T. C. *J. Am. Chem. Soc.* **1969**, *91*, 2985 - 2993.

Scheme 4

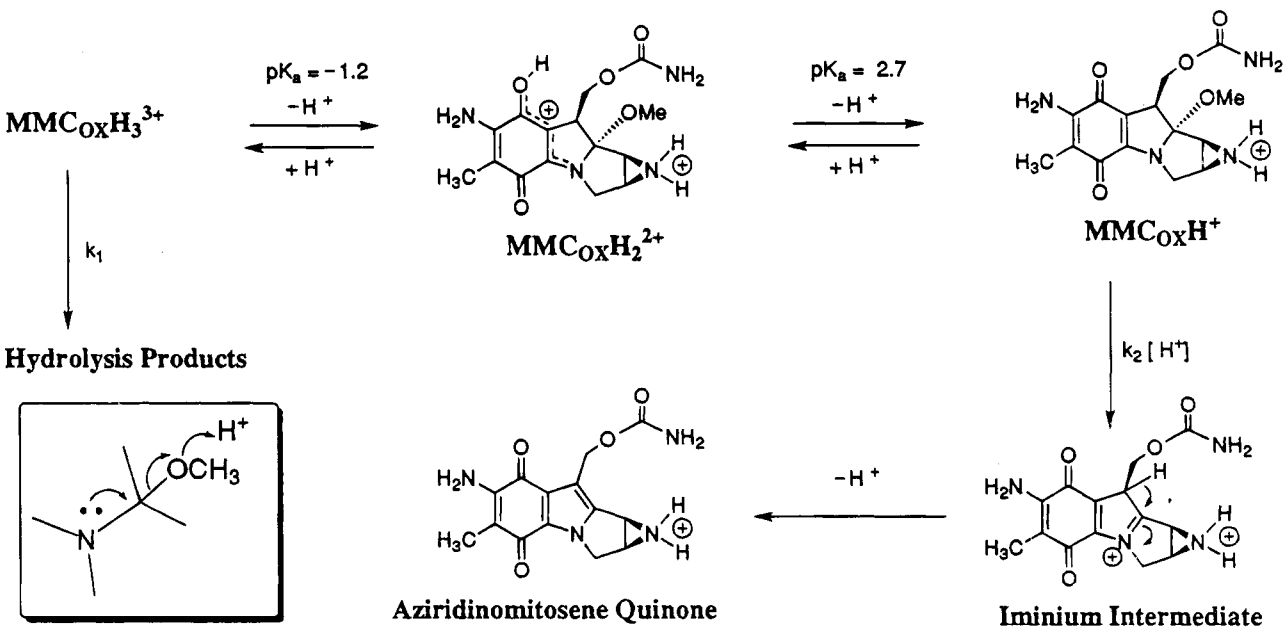

The oxidized species has a single pK_a for quinone protonation: pK_{a1} = −0.51. Two-electron reduction to the hydroquinone $\mathbf{1}_{red}$ results in the presence of three acid dissociations: pK_{a1} for the protonated 7-amino group, and pK_{a2} and pK_{a3} for acid dissociation from the hydroxyl groups. The relationship between the potential at a pH value (E_m) and the pH of the solution for the couple $\mathbf{1}_{ox}$/$\mathbf{1}_{red}$ is

$$E_m = E_o + \frac{RT}{nF}\ln\left(\frac{[\mathbf{1}_{red}]}{[\mathbf{1}_{ox}]}\right)$$

$$= E_o + \frac{RT}{nF}\ln\left(\frac{a_H^3 + a_H^2K_{a1} + a_HK_{a1}K_{a2} + K_{a1}K_{a2}K_{ae}}{a_H + K_{a1}}\right) \quad (4)$$

where $E_o = E_m$ at pH = 0, a_H is the proton activity determined with a pH meter, R = 8.314 volt Faraday K^{-1}, T = 298 °K, n = 2 (electrons), F (Faraday) = 96484 Coulombs mol^{-1}, and K_a (numerator) and K_a (denominator) are acid dissociation constants of the reduced and oxidized species respectively. Shown in Figure 2 is a plot of E_m vs pH data for the couple $\mathbf{1}_{ox}$/$\mathbf{1}_{red}$. The E_m data were determined from cyclic voltammograms, obtained in anaerobic aqueous buffers (μ = 1, NaClO$_4$), by taking the average of the anodic and cathodic potentials.

The voltammograms showed the ~30 mV difference between anodic and cathodic potentials expected for reversible two-electron transfer.[19] Furthermore, the voltammograms were highly symmetric in character (α = 0.5).[19] The reversibility and symmetry of the $\mathbf{1}_{ox}$/$\mathbf{1}_{red}$ couple suggested a well-behaved redox couple.

The E_m vs pH plot in Figure 2 clearly shows two inflections corresponding to pK_{a1} for acid dissociation form the protonated quinone ring of $\mathbf{1}_{ox}$ and pK_{a1} for acid dissociation form the protonated 7-amino group of $\mathbf{1}_{red}$. Inflections corresponding to acid dissociation from the hydroxyl groups of $\mathbf{1}_{red}$ are not seen in Figure 2. These acid dissociations have been observed in electron-deficient hydroquinones such as benzimidazoles (9.75),[10] imidazoquinazolines (8.54),[10] and quinazolines (7.8 and 10.60).[13] The relatively electron-rich $\mathbf{1}_{red}$ is expected to possess a pK_a for the first hydroxyl acid dissociation well above 10.

The data in Figure 2 were fit to eq 4 using the previously determined value of pK_{a1} = −0.51 (Scheme 3) for $\mathbf{1}_{ox}$ and pK_{a2} and pK_{a3} values > than 10 for $\mathbf{1}_{red}$. The value of pK_{a1} for $\mathbf{1}_{red}$ was the variable, and the best fit was obtained when this value was 5.70. The solid line in Figure 2 was generated from eq 4 substituted with the above pK_a values and E_o = 266 mV (NHE). The value of pK_{a1} = −0.51 is much lower than that measured for the protonated quinone ring of MMC$_{ox}$ (pK_{a2} = 2.7). The lower pK_a value of protonated $\mathbf{1}_{ox}$ is due to the presence of the indole ring rather than the electron-rich indoline ring of MMC$_{ox}$.

The MMC$_{ox}$/MMC$_{red}$ redox couple is less well behaved than the $\mathbf{1}_{ox}$/$\mathbf{1}_{red}$ couple, particularly in strong acid. One factor is the rapid reaction of MMC$_{red}$ above pH 5. (Hoey et al. measured a first-order rate constant of 1.2 s^{-1} for decomposition.[7]) Thus cyclic voltammograms of MMC$_{ox}$ below pH 5 showed a single cathodic potential corresponding to two-electron reduction of MMC$_{ox}$ to MMC$_{red}$ and at least two anodic potentials resulting from the reoxidation of MMC$_{red}$ and a decomposition product. The decomposition product had a lower anodic potential than MMC$_{red.}$ and is very likely a mitosene. Mitosene products are known to result from decomposition of MMC$_{red}$[20-23] and the mitosene analogue $\mathbf{1}_{ox}$ in fact possesses slightly lower redox potentials than MMC$_{ox}$ (compare E_o for $\mathbf{1}_{ox}$/$\mathbf{1}_{red}$ = 266 mV [NHE] and E_o for MMC$_{ox}$/MMC$_{red}$ = 302 [NHE], *vide infra*, Figure 3). Another complicating factor is the rapid hydrolysis of MMC$_{ox}$ in strong acid. Thus cyclic voltammograms show the formation of multiple anodic/cathodic waves corresponding to hydrolysis products. Repetitive scanning showed the eventual disap-

(17) Clark, W. M. *Oxidation-Reduction Potentials of Organic Systems*; Williams S. Wilkins: Baltimore, MD, 1960; Chapter 4.
(18) For examples of Complex Nernst–Clark equations see: Eberlein, G. A.; Bruice, T. C. *J. Am. Chem. Soc.* **1983**, *105*, 6685–6697.
(19) Bard, A. J.; Faulkner, L. R. *Electrochemical Methods*; Wiley: New York, 1980; pp 227–231.
(20) Han, I.; Kohn, H. *J. Org. Chem.* **1991**, *56*, 4648–4653.
(21) Li, V.-S.; Kohn, H. *J. Am. Chem. Soc.* **1991**, *113*, 275–283.
(22) Hong, Y. P.; Kohn, H. *J. Am. Chem. Soc.* **1991**, *113*, 4634–4644.
(23) Kohn, H.; Hong, Y. P. *J. Am. Chem. Soc.* **1990**, *112*, 4596–4598.

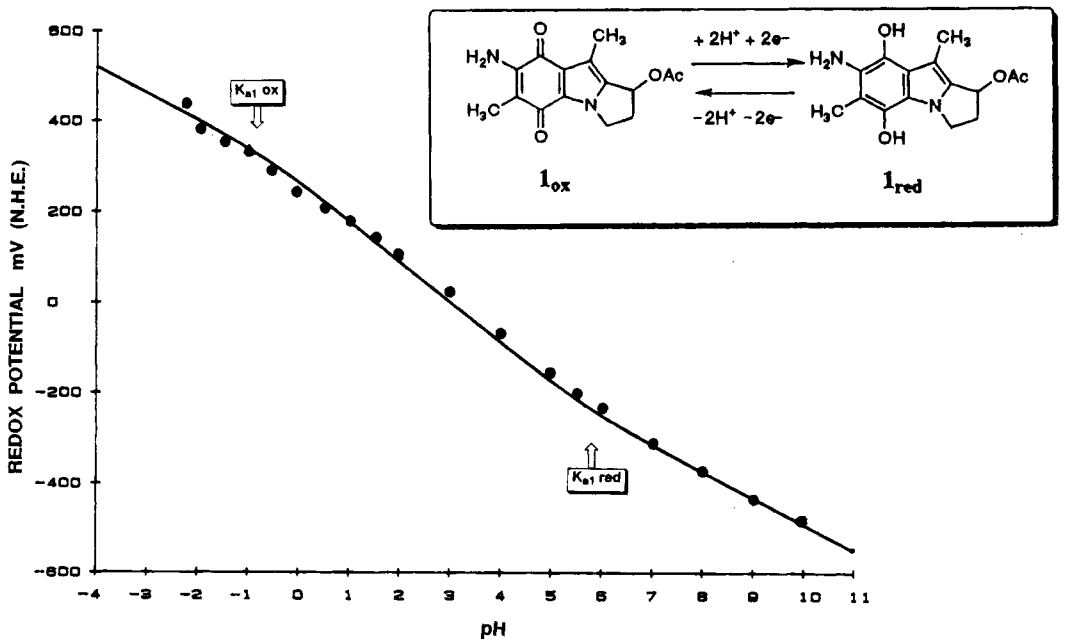

Figure 2. Plot of redox potential (NHE) vs pH for the $\mathbf{1_{ox}/1_{red}}$ redox couple. Potential data measured in anaerobic aqueous buffer (μ = 1.0, $NaClO_4$) at 25–26 °C.

pearance of the MMC_{ox}/MMC_{red} couple in strong acid. E_m values were obtained below pH 5 from the cathodic and anodic potentials for the MMC_{ox}/MMC_{red} couple, which could be distinguished from those of decomposition products. Above pH 5 the MMC_{ox}/MMC_{red} couple is well behaved and shows single cathodic and anodic waves and reversible (or pseudoreversible[19]) two electron-transfer. The observation is consistent with the relatively slow decomposition of MMC_{red} near neutrality reported by Hoey et al.[7]

The Nernst–Clark equation for the MMC_{ox}/MMC_{red} couple is provided in eq 5:

$$E_m = E_o + \frac{RT}{nF}\ln\left(\frac{[MMC_{red}]}{[MMC_{ox}]}\right)[MMC_{red}]/[MMC_{ox}] = \frac{a_H^5 + a_H^4K_{a1} + a_H^3K_{a1}K_{a2} + a_H^2K_{a1}K_{a2}K_{a3} + a_HK_{a1}K_{a2}K_{a3}K_{a4} + K_{a1}K_{a2}K_{a3}K_{a4}K_{a5}}{a_H^3 + a_H^2K_{a1} + a_HK_{a1}K_{a2} + K_{a1}K_{a2}K_{a3}} \quad (5)$$

where the values of the constants are the same as previously cited, see eq 4, and K_a (numerator) and K_a (denominator) are acid dissociation constants of MMC_{red} and MMC_{ox}, respectively. For MMC_{ox} the values of $pK_{a1} = -1.23$ and $pK_{a2} = 2.72$ were substituted into eq 5 and pK_{a3} (the protonated aziridino nitrogen dissociation constant) was the variable. For MMC_{red} the values of pK_{a2} = 5.1 to 6.1, and pK_{a4} and $pK_{a5} > 10$ were substituted into eq 5 and pK_{a1} and pK_{a3} were the variables. The setting of the hydroquinone hydroxyl ionizations of MMC_{red} (pK_{a4} and pK_{a5}) greater than 10 is valid on the basis of the experience with the $\mathbf{1_{ox}/1_{red}}$ couple, which did not show the presence of these ionizations in the pH range studied.

Fitting E_m vs pH data shown in Figure 3 for the MMC_{ox}/MMC_{red} couple to eq 5 provided the following values for the variable pK_a terms: pK_{a3} for MMC_{ox} = 7.6 and pK_{a1} and pK_{a3} for MMC_{red} = 1.4 and ~9 respectively. The value of pK_{a2} for MMC_{red} was varied between 5.1 and 6.1, typical pK_a values for protonated amino hydroquinones.[10–12] The better fit was obtained with pK_{a2} = 6.1, which was used to generate the solid line in Figure 3. The solution, pK_{a1} = 1.4 for MMC_{red}, can be seen as an inflection in the E_m vs pH data. An inflection for pK_{a3} = 7.6 (MMC_{ox}) is also apparent in Figure 3. However, the solution pK_{a3} = 9 for MMC_{red} is less certain due to the proximity of pK_{a3} for MMC_{ox}. The influence of both pK_{a3} values on E_m is relatively slight since the acid dissociation of the protonated aziridino nitrogen is influenced by the quinone or hydroquinone only via through-bond effects. However, the study of MMC_{red} reactions in anaerobic buffer described in the next section clearly shows a pK_a value of 9.10 for the protonated aziridino nitrogen.

Inductive effects are very likely responsible for the lower pK_{a3} value of MMC_{ox} (7.6) compared to the pK_{a3} value of MMC_{red} (9.1). The 1.5 pK_a unit difference is small compared to the 3-unit difference in pK_{a2} observed between MMC_{ox} and MMC_{red} due to conjugation of the protonated center with the quinone ring.

The pH rate profile of Hoey et al.[7] (Figure 7 of this reference) will now be interpreted in terms of the pK_a assignments of MMC_{red}. Their profile shows protonated MMC_{red} (pK_a = 5.1) reacting at 1.2 s^{-1} and the deprotonated form reacting at 0.015 s^{-1}. The observed products were aziridino ring-opened mitosenes as well as unreacted MMC_{ox} (see HPLC trace in Figure 3 of ref 7). The apparent first-order formation of these products suggested that MMC_{red} proceeded directly to these products. In this report it is suggested the pH rate profile of Hoey et al. pertains to the elimination of methanol from MMC_{red} to afford the aziridinomitosene hydroquinone as shown in Scheme 5. This hydroquinone species is then converted to the observed aziridino ring-opened products. The sequential elimination of methanol and aziridino ring opening has been reported for both MMC_{ox}[5] and MMC_{red}.[20–23] In fact Han and Kohn[20] were able to isolate the aziridinomitosene quinone upon reduction of MMC_{ox} and reoxidation. In the present study, isolation of the aziridinomitosene quinone was also possible by combining MMC_{red} with anaerobic aqueous buffer followed

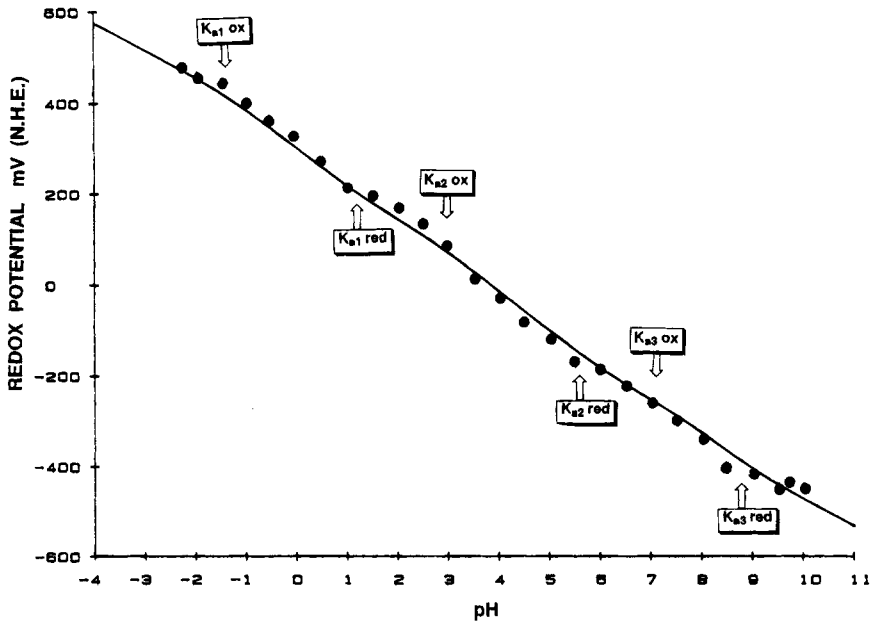

Figure 3. Plot of redox potential (NHE) vs pH for the MMC_{ox}/MMC_{red} redox couple. Potential data measured in anaerobic aqueous buffer (μ = 1.0, $NaClO_4$) at 25–26 °C.

Scheme 5

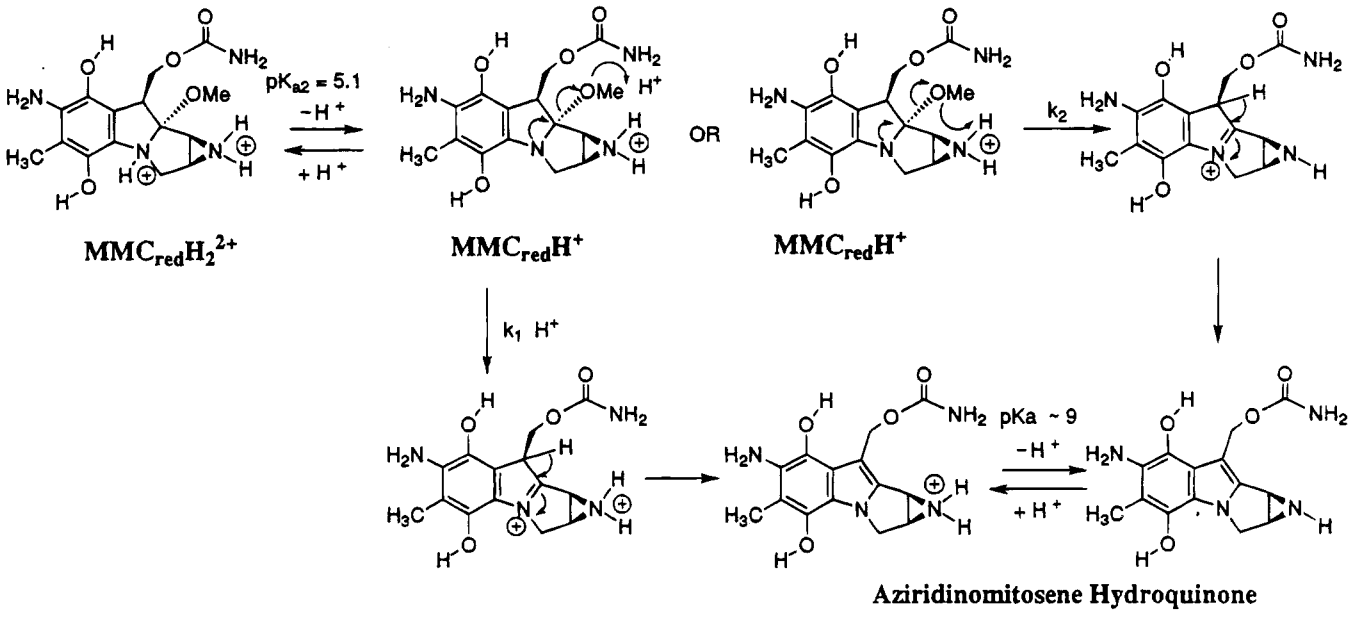

immediately by aeration (*vide infra*, Reaction of MMC_{red} in Anaerobic Aqueous Buffer).

The pK_a of 5.1 to 6.1 is attributed to acid dissociation from the indoline nitrogen of MMC_{red} (pK_{a2}). In fact, the pK_a values for acid dissociation from protonated amino hydroquinones are very close to this range of values (examples are pK_a = 4.7,[11] 4.58,[10] and 6.02[12]). Protonation of the indoline nitrogen prevents participation of the lone pair in methoxide elimination from MMC_{red} H_2^{2+} (Scheme 5). Specific acid-catalyzed elimination of methanol therefore occurs from $MMC_{red}H^+$ at k_1 M^{-1} s^{-1}. The protonated aziridino nitrogen can act as an internal general acid and facilitate the elimination of methanol at k_2 s^{-1} from MMC_{red} H^+ (Scheme 5). McClelland and Lam[5] likewise observed both specific and general acid-catalyzed elimination of methanol from MMC_{ox}. Significantly the mechanisms of methanol elimination from MMC_{ox} and MMC_{red} (Schemes 4 and 5 respectively) are virtually identical.

The rate law for the mechanism in Scheme 5 is shown in eq 6:

$$k_{obsd} = \frac{k_1 a_H K_{a2} + k_2 K_{a2}}{a_H + K_{a2}} \qquad (6)$$

This equation has the same form as that presented by Hoey et al.,[7] although the interpretation of constants is different: k_1 is 1.5 × 10^5 M^{-1} s^{-1} for the specific acid-catalyzed elimination of methanol from MMC_{red} H^+ and k_2 is 0.015 s^{-1} for the spontaneous elimination of methanol from MMC_{red} H^+. Comparison of k_1 with the same constant determined for acid-catalyzed elimination of methanol from MMC_{ox} H^+ (k_1 = 1.5 M^{-1} s^{-1}) reveals that reductive activation results in a 100000-fold increase in the rate constant for methanol elimination.

If the protonated aziridino nitrogen of $MMC_{red}H^+$ does facilitate the loss of methanol, then k_{obsd} should decrease at pH values >9 due to formation of neutral MMC_{red}. The

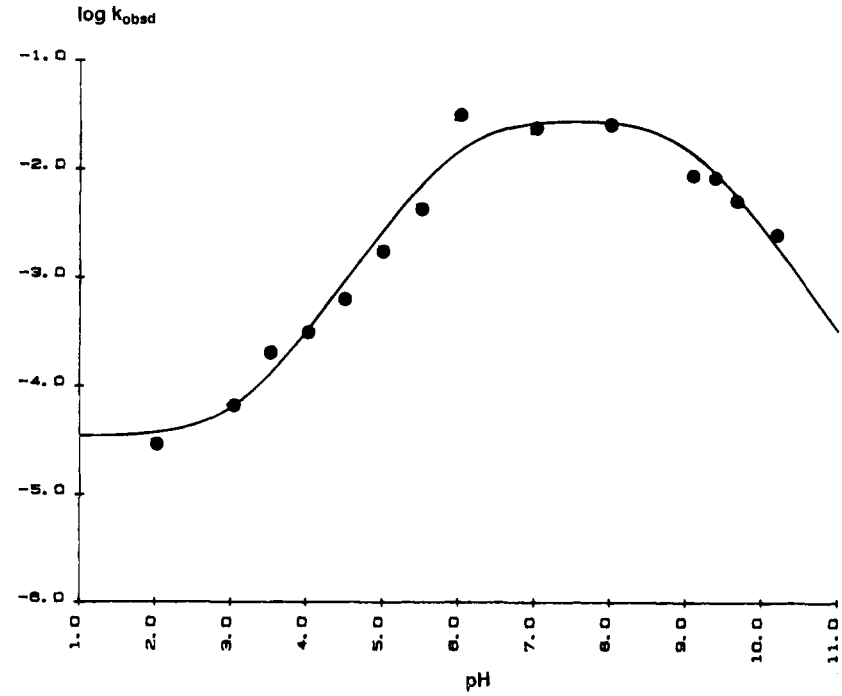

Figure 4. Plot of log k_{obsd} vs pH for the hydrolysis of MMC_{red} in anaerobic buffer (μ = 1.0, KCl) at 30.0 ± 0.2 °C.

data of Hoey et al. did not extend to pH values > 8, however. A new kinetic study of the MMC_{red} reaction in anaerobic aqueous buffer did show the expected decreasing k_{obsd} values at pH > 9 with a pK_a = 9.1 in the pH rate profile (*vide infra*, following section).

Reaction of MMC_{red} in Aqueous Buffer. A pH rate profile (Figure 4) was obtained for the reaction of MMC_{red} in anaerobic aqueous buffer. This profile clearly shows that the pK_a for the protonated aziridino nitrogen is 9.1. The results of this study are consistent with the formation of a carbocation species upon aziridino ring opening as proposed by Han and Kohn.[20]

Catalytic reduction of MMC_{ox} in dimethyl sulfoxide containing a small amount of water (≤25%) afforded MMC_{red} without any significant elimination of methanol or ring opening. Reoxidation of the MMC_{red} stock solution by addition of air, followed by evaporation to dryness under high vacuum, afforded pure MMC_{ox}. (^{1}H NMR matched that of authentic material.) Addition of the dimethyl sulfoxide stock of MMC_{red} to anaerobic aqueous buffers resulted in a first-order absorbance decrease at 350 nm for ~5 half-lives. The log k_{obsd} vs pH data thus obtained are shown in Figure 4.

The data in Figure 4 represent two processes: At pH values <6, the reaction followed was the ring opening of the aziridinomitosene hydroquinone. At pH values > 6, the reaction followed was the loss of methanol from MMC_{red}. Hoey et al. observed that MMC_{red} eliminates methanol at 1.2 s^{-1} at pH values < 5.1. Therefore additions of MMC_{red} to anaerobic aqueous buffers held at pH values < 6 would result in rapid formation of the aziridinomitosene hydroquinone. Isolation studies at pH 4.0 showed this to be the case. When MMC_{red} was added to anaerobic pH 4.0 acetate buffer, followed immediately by aeration and extraction with chloroform, only the aziridinomitosene quinone was obtained as the product. This product possessed an ^{1}H NMR spectrum in dimethyl sulfoxide-d_6 like that reported by Han and Kohn.[20] Noteworthy features of this spectrum are the singlet at 5.02 ppm for the C-10 methylene, indicating that methanol elimination had occurred, and the presence of an upfield triplet at 2.18 ppm (J = 7.5 Hz) for the aziridino NH coupled to the C-1 and C-2 methine protons. The chemical shift of the triplet matched that of the aziridinomitosene quinone with the aziridino N−H in the anti conformation. The *syn* isomer reported by Han and Kohn[20] was not obtained on the basis of the absence of a second upfield aziridino N−H triplet. From pH 6 to 8, the data in Figure 4 nearly matches those reported by Hoey et al., k_{obsd} = 0.015 s^{-1} reported and k_{obsd} = 0.035 s^{-1} measured in this study. The products Hoey et al.[7] observed in this pH range are the result of both methanol loss and opening of the aziridino ring without any apparent buildup of the aziridinomitsene intermediate.

The rate law for the mechanism in Scheme 6 is shown in eq 7:

$$k_{obsd} = \frac{k_3 a_H^{\,2} + k_2\, a_H K_{a4}}{a_H^{\,2} + a_H K_{a4} + K_{a4} K_{a3}} \qquad (7)$$

Fitting eq 7 to the data in Figure 4 provided the following solution which was used to generate the solid line in this figure: $k_3 = 3.61 \times 10^{-5}$ s^{-1}, k_2 = 0.0353 s^{-1}, pK_{a4} = 6.10, and pK_{a3} = 9.10. The value of pK_{a4} is nearly identical to that determined for the protonated 7-amino group of $\mathbf{1}_{red}$ (pK_a = 5.7) and the value of pK_{a3} is typical of a protonated aziridine nitrogen.[9]

The data in Figure 4 is discussed below in conjunction with the mechanism in Scheme 6. Rapid specific acid-catalyzed formation of the aziridinomitosene below pH 6 (at k_1 M^{-1} s^{-1}) is followed by slow opening (k_3) of the aziridino group to afford the carbocation species. Han and Kohn[20] have previously proposed that aziridino ring opening leads to a carbocation intermediate. Protonation of the 7-amino group of the aziridinomitosene hydroquinone would slow carbocation formation as a result of unfavorable electrostatic effects. Above pH 6, the 7-amino group is neutral and carbocation formation at k_4 s^{-1} should be very favorable. The data of Hoey et al. show that MMC_{red} is converted to aziridino ring opened products without buildup of an intermediate, which suggests

Scheme 6

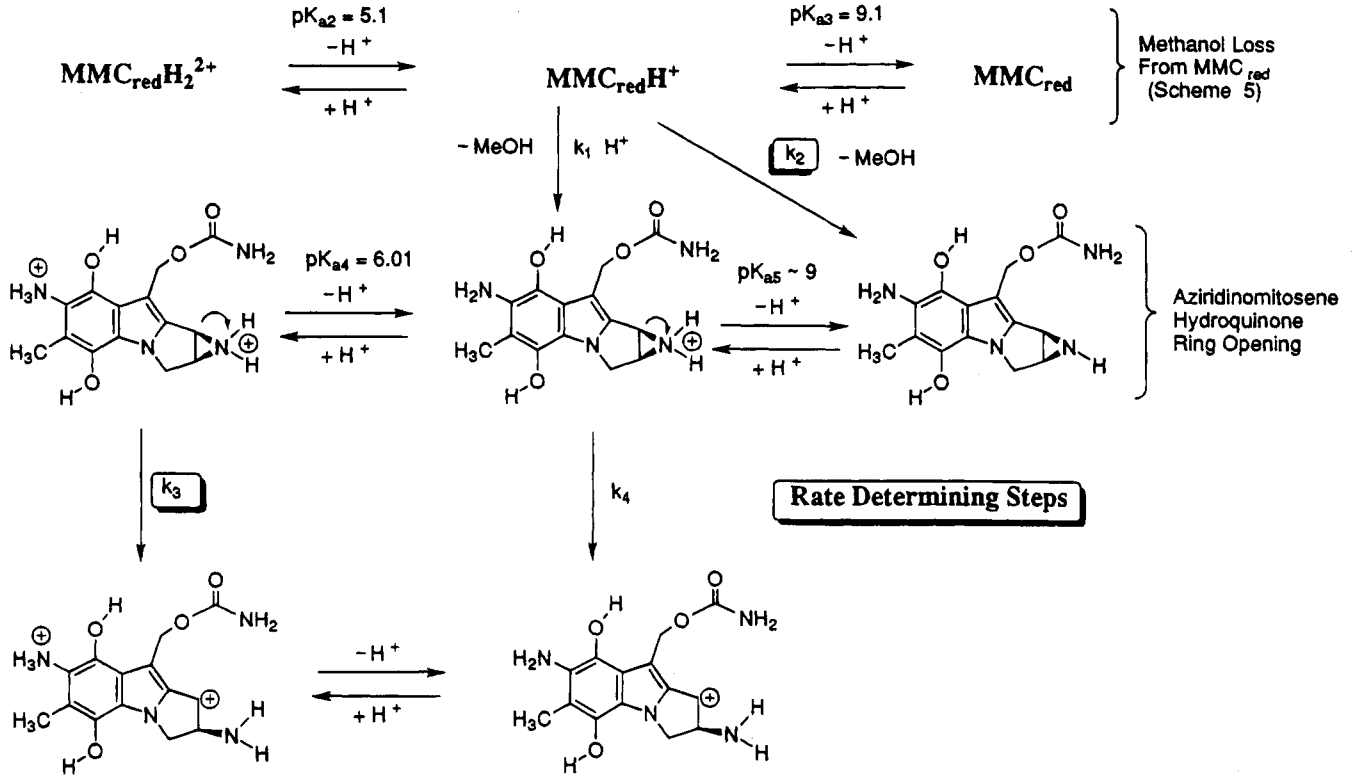

Mitosene Hydroquinone Carbocation

that $k_4 \geq k_2$ in Scheme 6. Finally, above pH 9, acid dissociation to neutral MMC_{red} results in decreasing k_{obsd} values with increasing pH. The neutral form of MMC_{red} cannot undergo specific acid- or general acid-catalyzed elimination and should be stable in solution. In fact, MMC_{red} dissolved in dimethyl sulfoxide (this report) and in pyridine[24] is stable. The aziridinomitosene hydroquinone should also be stable above pH 9 assuming a p$K_{a5} \approx 9$ for the protonated aziridino nitrogen. Han and Kohn[20] have observed a decrease in the rate of aziridino ring opening in methanolic buffers upon increasing the pH to ~8.5.

Fate of the Mitosene Analogue 1_{red}. The hydrolysis of the mitosene analogue 1_{red} is discussed below in conjunction with Scheme 7 and Figure 5. The mechanism of hydrolysis is similar to that proposed for the aziridinomitosene hydroquinone in Scheme 6 and for other mitosenes bearing an acetate leaving group in the 1-position.[25] Thus, rate-determining elimination of acetate from 1_{red} affords a carbocation, which is then converted to an alkylating quinone methide species (*vide infra*, Fate of the Mitosene Carbocation). The disappearance of 1_{red} in anaerobic aqueous buffer was followed spectrophotometrically at 320 nm. Absorbance vs time plots were first order in character and rate constants were obtained by fitting these plots to a single exponential decay. The first-order rate constants were found to be highly dependent on the concentration of buffer below pH 7 and therefore buffer dilutions were carried out in this pH range. Plots of k_{obsd} for the disappearance of 1_{red} vs total buffer concentration at constant pH provided the lyate-only k_{obsd} value upon extrapolation to zero buffer. Shown in Figure 5 is a log k_{obsd} vs pH plot for the lyate-catalyzed processes.

Scheme 7

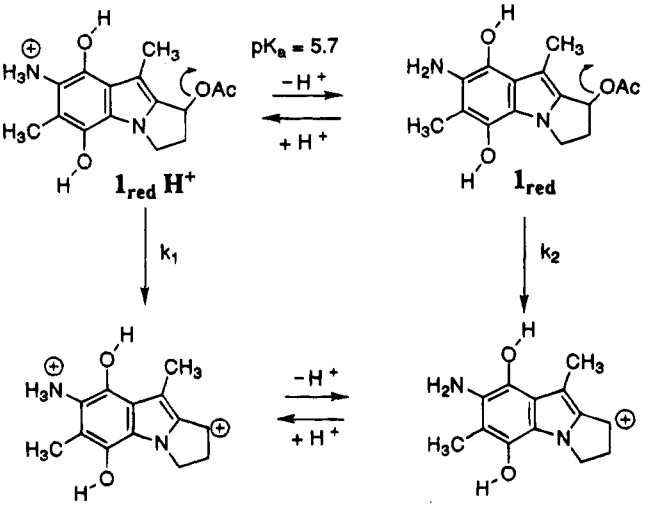

Mitosene Hydroquinone Carbocation

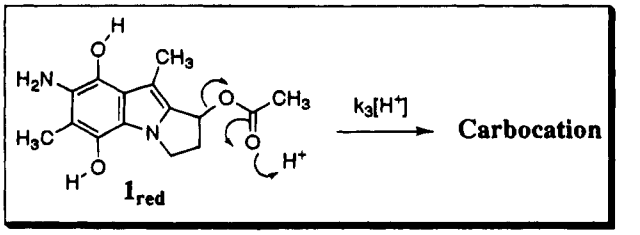

Mechanistic interpretations of the data in Figure 5 are provided in Scheme 7. Above pH 5.70, where 1_{red} exists in the neutral form, the spontaneous loss of acetate from

(24) (a) Danishefsky, S. J.; Ciufolini, M. *J. Am. Chem. Soc.* **1984**, *106*, 6424–6425. (b) Danishefsky, S. J.; Egbertson, M. *J. Am. Chem. Soc.* **1986**, *108* 4648–4650.

(25) Maliepaard, M.; de Mol, N. J.; Janssen, L. H. M.; Hoogvliet, J. C.; van der Neut, W.; Verboom, W.; Reinhoudt, D. N. *J. Med. Chem.* **1993**, *36*, 2091–2097.

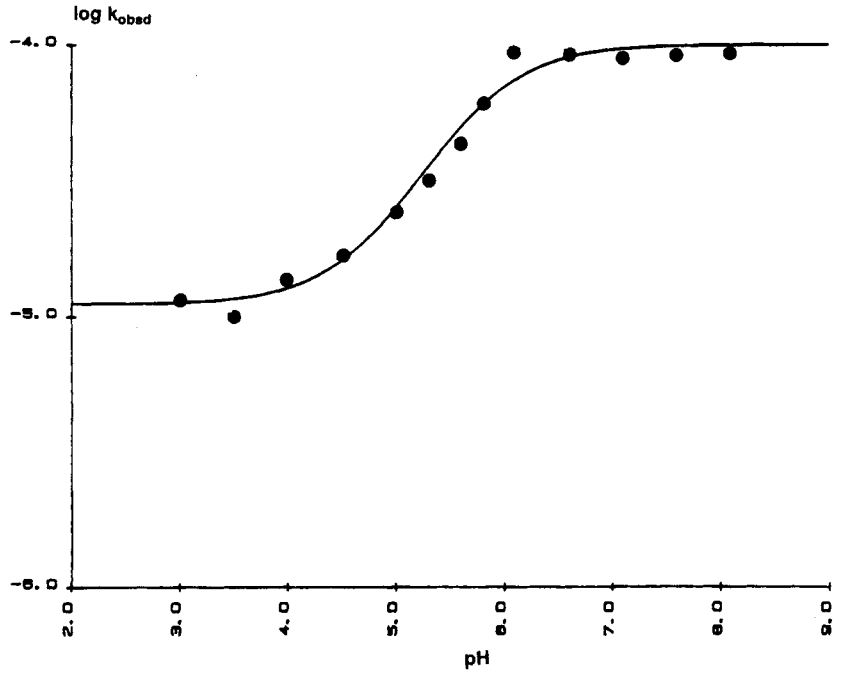

Figure 5. Plot of log k_{obsd} (lyate) vs pH for the hydrolysis of $\mathbf{1}_{red}$ in anaerobic buffer (μ = 1.0, KCl) at 30.0 ± 0.2 °C.

$\mathbf{1}_{red}$ occurs to afford the carbocation species resulting in the observed high pH (>6) plateau. Below pH 5.70, where $\mathbf{1}_{red}$ is protonated, the observed plateau can be interpreted as loss of acetate from $\mathbf{1}_{red}\mathbf{H}^+$ or the specific acid-catalyzed loss of acetate from $\mathbf{1}_{red}$ (inset of Scheme 7). These possibilities can be distinguished by considering electrostatic effects and the presence of buffer catalysis. The rate law provided in eq 8 considers the spontaneous loss of acetate from $\mathbf{1}_{red}$ and $\mathbf{1}_{red}\mathbf{H}^+$:

$$k_{obsd} = \frac{a_H k_1 + K_a k_2}{a_H + K_a} \quad (8)$$

when k_1, k_2, and K_a are constants in Scheme 7. Fitting eq 8 to the data in Figure 5 provides $k_1 = 1.1 \times 10^{-5}$ s^{-1}, $k_2 = 1.0 \times 10^{-4}$ s^{-1}, and pK_a = 5.7. This solution was used to generate the solid line in Figure 5. The problems with this mechanism are the absence of a significant electrostatic effect on dication formation ($k_2/k_1 = 11$) and the absence of a process which would explain buffer catalysis. The alternative to dication formation is to consider specific acid-catalyzed loss of acetate from $\mathbf{1}_{red}$, eq 9:

$$k_{obsd} = \frac{a_H K_a k_3 + K_a k_2}{a_H + K_a} \quad (9)$$

This equation is kinetically indistinguishable from eq 8 and could also be used to generate the solid line in Figure 5. The solution obtained by fitting eq 9 to the data in Figure 5 is $k_2 = 1.0 \times 10^{-4}$ s^{-1}, $k_3 = 6$ M^{-1} s^{-1}, and pK_a = 5.7. This alternative mechanism explains the presence of buffer catalysis since general acids as well as specific acids will assist in the elimination of acetate.

Other mechanistic possibilities for the anaerobic hydrolysis of $\mathbf{1}_{red}$ are discussed below. One possibility is disproportionation between the quinone formed in the course of hydrolysis ($\mathbf{5}_{ox}$, Scheme 8) and unreacted $\mathbf{1}_{red}$. In order to preclude this reaction, the disappearance of $\mathbf{1}_{red}$ was followed starting with a low initial concentration of 3×10^{-5} M, at which the absorbance vs time plots were first order in character for up to 10 half-lives. Another mechanistic possibility is the presence of acid or base hydrolysis of the acetate group of $\mathbf{1}_{red}$. The pH rate profile in Figure 5 shows a plateau above pH 5.7, which indicates the spontaneous loss of acetate from neutral $\mathbf{1}_{red}$. If a $B_{AC}2$ mechanism was occurring, the basic region of the pH rate profile would have a slope of +1. Indeed, our mechanistic conclusion regarding the elimination of acetate from $\mathbf{1}_{red}$ (Scheme 7) is similar to that reported for 1,10-diacetoxymitosenes.[25]

Fate of the Mitosene Carbocation. This section addresses the fate of the carbocation species arising from the mitosene model system $\mathbf{1}_{red}$. The products resulting from anaerobic hydrolysis of $\mathbf{1}_{red}$, isolated under aerobic conditions, are $\mathbf{4}_{ox}$ and $\mathbf{5}_{ox}$ shown in the insets of Scheme 8. These respective products represent nucleophilic (water) and electrophilic (proton) trapping of the carbocation and quinone methide species arising from $\mathbf{1}_{red}$. Water addition to the carbocation or quinone methide affords $\mathbf{4}_{red}$, which is converted to $\mathbf{4}_{ox}$ upon workup. Proton trapping of the quinone methide anion affords the quinone $\mathbf{5}_{ox}$ directly. Both $\mathbf{4}_{red}$ and $\mathbf{5}_{ox}$ are formed during the first-order disappearance of $\mathbf{1}_{red}$ in anaerobic buffer. Thus, rate-determining loss of acetate (Scheme 7) is followed by trapping of the steady state carbocation and quinone methide species. In a second first-order process, which is much slower (10-fold) than the initial first-order process, $\mathbf{4}_{red}$ and $\mathbf{5}_{ox}$ decompose to uncharacterized polar products. The mitosene $\mathbf{1}_{ox}$ even undergoes slow decomposition ($\sim 1 \times 10^{-6}$ s^{-1}) in buffer. In order to differentiate between carbocation and quinone methide trapping, the nucleophile and proton trapping product yields were determined as a function of pH. Below pH 7, the yield of the nucleophile-trapping product was far greater than the proton-trapping product: 37% $\mathbf{4}_{ox}$ isolated at pH 5 and 6 with a trace of $\mathbf{5}_{ox}$. At pH 7 and above the proton-trapping product was more evident: pH 7, 36% $\mathbf{4}_{ox}$ and 21% $\mathbf{5}_{ox}$; pH 7.5, 36% $\mathbf{4}_{ox}$ and 22% $\mathbf{5}_{ox}$; pH 8, 32% $\mathbf{4}_{ox}$ and 16% $\mathbf{5}_{ox}$. The low mass balances are due to the decomposition of quinone products as stated above. Evidence for formation of $\mathbf{4}_{red}$ and $\mathbf{5}_{ox}$ at the conclusion

Scheme 8

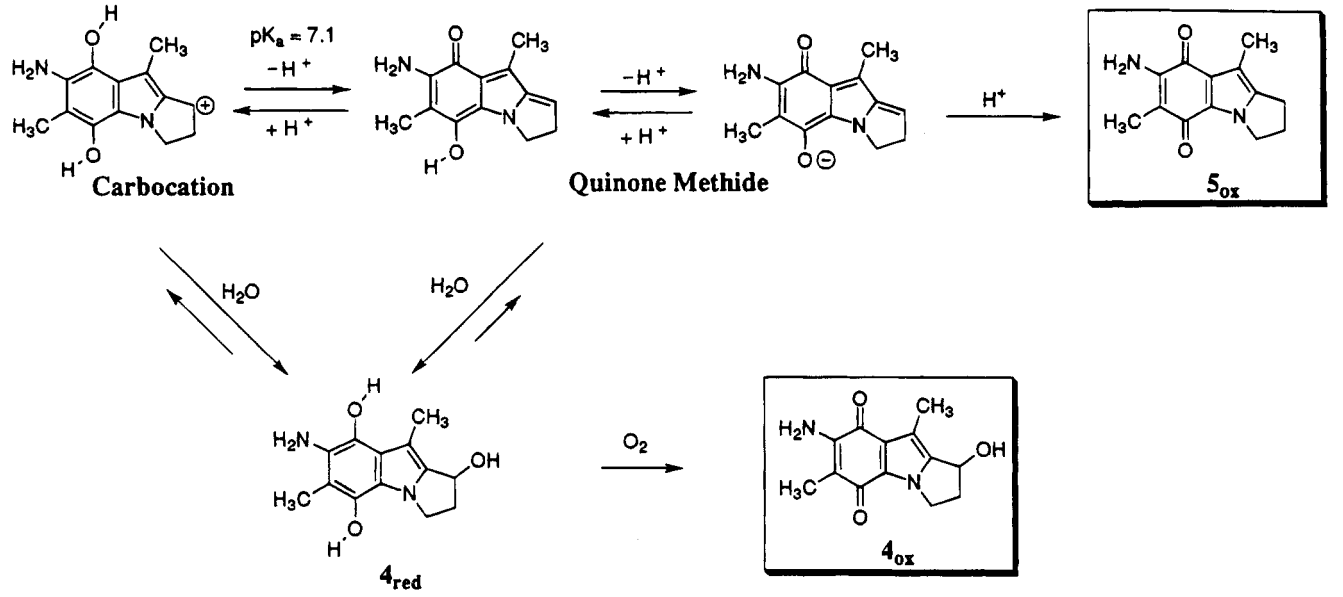

of the first-order disappearance of $\mathbf{1}_{red}$ was obtained from UV–visible spectroscopy of low concentration (3×10^{-5} M) reaction mixtures. The buildup of quinone $\mathbf{5}_{ox}$ is apparent at 570 nm (see Figure 6). Addition of air results in an additional absorbance increase at 570 nm corresponding the air oxidation of $\mathbf{4}_{red}$ to $\mathbf{4}_{ox}$. The total absorbance at 570 nm corresponds to the near quantitative conversion of $\mathbf{1}_{red}$ to the observed products.

The findings cited above reflect those obtained with a benzimidazole-based quinone methide system[26,27] as well as with the mitosene-based quinone methide.[28] Evidence was obtained consistent with an equilibrium between the benzimidazole carbocation and the corresponding quinone methide pK_a = 5.5.[27] The benzimidazole quinone methide species traps both nucleophiles and a proton, whereas the carbocation species traps nucleophiles. Consequently, there is a pH dependence for product formation. The fate of the mitosene carbocation and quinone methide species in Scheme 8 is interpreted below in light of the results of the benzimidazole study.

As shown in Scheme 8 the mitosene carbocation (pK_a = 7.1) traps water to afford $\mathbf{4}_{red}$ as the major product. Above the carbocation pK_a, the quinone methide species traps both water and a proton. The quinone methide anion traps the proton whereas the neutral quinone methide traps water. Since both processes essentially occur from neutral quinone methide, the ratios of water and proton trapping products are independent of pH (see refs 26 and 27 for further discussion). The mitosene carbocation pK_a was determined on the basis of the concentration of $\mathbf{5}_{ox}$ (λ_{max} = 570 nm) at the conclusion of the first-order disappearance of $\mathbf{1}_{red}$ under anaerobic conditions. The plot of absorbance at 570 nm vs pH in Figure 6 was fit to the spectrophotometric pK_a equation (see Experimental Section). The solution, pK_a = 7.1 ± 0.2, was used to generate the solid line in this figure. Above pK_a = 7.1 the formation of $\mathbf{5}_{ox}$ is independent of pH producing the plateau in absorbance at 570 nm. Below pK_a = 7.1, very little $\mathbf{5}_{ox}$ is actually formed but trailing of the product UV–visible spectrum produces some absorbance at 570 nm. It is important to point out that $\mathbf{5}_{ox}$ can form below pK_a = 7.1 as the thermodynamic product. Thus, $\mathbf{4}_{red}$ is the kinetic product below pK_a = 7.1, but the slow loss of water from $\mathbf{4}_{red}$ to afford the carbocation in Scheme 8 lead to the irreversible formation of $\mathbf{5}_{ox}$.

The pK_a of 7.1 for the mitosene carbocation acid dissociation is higher than that observed for the benzimidazole system due to the more electron-rich character of the mitosene system. Usually protonated carbonyl oxygen possess pK_a values in the H_o region (negative pK_a values).[29] However, if protonation of a quinonoid or benzenoid system to afford an aromatic cation is very favorable the protonated species would possess a pK_a near neutrality. For example, the C-protonation of heptalene to afford an aromatic cation has a pK_a > 7.[30]

The mechanistic conclusions stated above can be applied to the mitosene carbocation derived from mitomycin C. Thus, below pH 7.1, the alkylating agent is a mitosene carbocation and above this pH value the alkylating agent is a quinone methide. Schiltz and Kohn in fact observed a pH dependence for proton trapping (p$K_a \approx 7$) similar to that illustrated in Figure 6 (Figure 3 of ref 28). Their interpretation of the pH dependence for product formation is based on acid dissociation from the quinone methide to afford the anion. However, studies in this laboratory[26,27] showed that this kind of acid dissociation could not be responsible for the product differences observed with pH.

Conclusions

A total of six pK_a values were determined for the MMC_{ox}/MMC_{red} redox couple. The pK_a values obtained reflect acid dissociation constants observed for similar systems in the literature in contrast to the anomalous assignments previously reported for the MMC_{ox}/MMC_{red} couple. Acid dissociations from the protonated aziridino nitrogen of MMC_{ox} and MMC_{red} were previously assigned as 2.7 to 3[4–6] and 5.1,[7] respectively. These values are abnormally low for a protonated aziridine nitrogen pK_a. The values for these respective acid dissociations obtained in this study are 7.6 and 9.1. The pK_a values previously determined for MMC_{ox} and MMC_{red}, 2.7 and

(26) Skibo, E. B. *J. Org. Chem.* **1986**, *51*, 522–527.
(27) Skibo, E. B. *J. Org. Chem.* **1992**, *57*, 5874–5878.
(28) Schiltz, P.; Kohn, H. *J. Am. Chem. Soc.* **1993**, *115*, 10510–10518.
(29) Steward, R.; Yates, K. *J. Am. Chem. Soc.* **1958**, *80*, 6355–6359.
(30) Dauben, H. J., Jr.; Bertelli, D. J. *J. Am. Chem. Soc.* **1961**, *83*, 4657–4659.

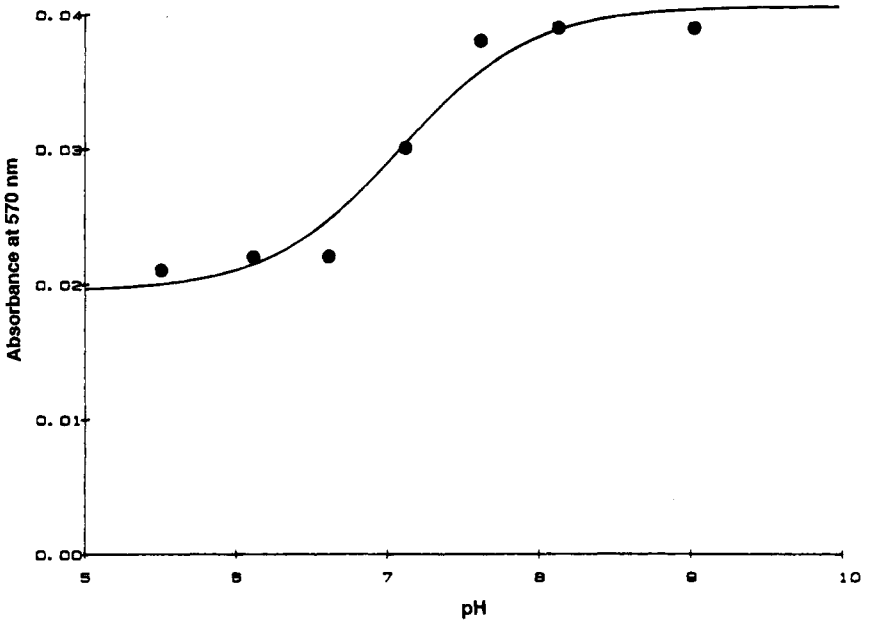

Figure 6. Plot of absorbance at 570 nm obtained at the conclusion of the initial first-order reaction vs pH for the hydrolysis of $\mathbf{1}_{red}$ in anaerobic buffer (μ = 1.0, KCl) at 30.0 ± 0.2 °C.

5.1 to 6.1 respectively, are now assigned to acid dissociation from the protonated indoline nitrogen. The acid dissociations for the protonated quinone of MMC_{ox} (-1.2) and the protonated 7-amino group of MMC_{red} (1.2) were also determined.

The above pK_a determinations were incorporated into previously reported mechanistic results. It is concluded that indoline nitrogen protonation prevents the elimination of methanol from MMC_{ox} or MMC_{red} since the nitrogen lone pair cannot be utilized in the elimination process. The elimination of methanol occurs from MMC_{ox} and MMC_{red} by a specific acid-catalyzed process similar to that previously reported for MMC_{ox} by McClelland and Lam.[5] There is a 100000-fold increase in the second-order rate constant for specific acid-catalyzed elimination of methanol when MMC_{ox} is reduced to MMC_{red}.

The kinetics of MMC_{red} hydrolysis was studied in anaerobic aqueous buffer. The pK_a value of the protonated aziridino group (9.1) was clearly observed in the pH rate profile for hydrolysis. Conclusions from this kinetic study are (1) a mitosene carbocation intermediate is formed as proposed by Han and Kohn;[20] and (2) the pK_a value of the protonated aziridino nitrogen is not anomalously low. The model mitosene hydroquinone, bearing an acetate leaving group ($\mathbf{1}_{red}$) likewise hydrolyzed via a carbocation intermediate.

The final part of this report deals with the fate of the mitosene carbocation formed from $\mathbf{1}_{red}$. It is concluded that a carbocation/quinone methide equilibrium exists in anaerobic buffer, pK_a = 7.1. The carbocation is the major species below pH 7.1 and therefore nucleophile trapping products are observed in this pH range. Above pH 7.1 the quinone methide is the predominate species and therefore both nucleophile and electrophile (proton) trapping products are observed in this pH range. These results reflect those obtained with a benzimidazole-based quinone methide system[26,27] as well as with the mitosene quinone methide derived from mitomycin C.[28]

Experimental Section

Mitomycin C (MMC_{ox}) was purchased from Sigma Chemical Company combined with sodium chloride. Elemental analyses of new compounds were performed by Atlantic Microlab Inc., Norcross, GA. All analytically pure compounds were dried under high vacuum in a heating pistol with refluxing methanol. Melting points are uncorrected and decomposition points were characterized by color darkening without complete melting. All TLC was run with Merck silica gel 60 (F_{254}) plates and employing a variety of solvents. IR spectra were taken as KBr and NaCl thin film pellets; the strongest IR absorbances are reported. Both ^1H and ^{13}C NMR spectra were taken on a 300-MHz spectrometer; chemical shifts of proton spectra are reported relative to TMS. Mass spectral measurements were made with a low-resolution instrument in the electron impact mode.

Kinetic Studies. The kinetic studies were carried out in buffers prepared with doubly distilled water and adjusted to μ = 1.0 with KCl. The following buffer systems were employed to hold pH: HCl/water, formic acid/formate (pK_a = 3.6), acetic acid/acetate (pK_a = 4.55), phosphate monobasic/phosphate dibasic (pK_a = 6.50), and boric acid/borate (pK_a = 9.2). These pK_a values were obtained at 30.0 ± 0.2 °C in μ = 1.0 (KCl) aqueous solutions. Measurements of pH were made with a Radiometer GK2401C combination electrode.

A stock solution of MMC_{ox} was obtained by dissolving the sodium chloride mixture supplied to Sigma in the appropriate amount of dimethyl sulfoxide and filtering through a Millex-SR 0.5 μm filter to remove the sodium chloride. The MMC_{ox} stock was used in kinetic studies of MMC_{ox} hydrolysis (Figure 1), MMC_{ox} pK_a determination, and in E_m determination (Figure 3). Kinetic studies of MMC_{ox} hydrolysis were carried out by adding 50 μL of dimethyl sulfoxide stock to 2.95 mL of buffer and collecting absorbance vs time data on a UV−vis spectrophotometer in thermostated cells held at 30.0 ± 0.2 °C. These data were then computer fit to a single first-order rate law.

The dimethyl sulfoxide stock solution of MMC_{red} was prepared as follows. To a solution of 2 mg (0.006 mmol) of MMC_{ox} in 3 mL of dimethyl sulfoxide containing up to 25% water was added 1.0 mg of 5% Pd on carbon followed by degassing with argon for 10 min. The anaerobic reaction mixture purged with H_2 gas for 2 min resulting in disappearance of the purple color. The presence of water in the dimethyl sulfoxide stock solution was required for rapid reduction of MMC_{ox}. In reagent-grade dimethyl sulfoxide, reduction took up to 12 min. The reduced reaction mixture was placed in an N_2 glove box and filtered through a Millex-SR 0.5 μm filter to remove the catalyst. The filtrate (50 μL) was added to 2.95 mL of anaerobic buffer and the absorbance (350 nm) vs time data obtained at 30.0 ± 0.2 °C with a UV−vis spectrometer for ~5 half-lives. The first-order reaction was followed by a

slow reaction which has 100-fold lower rate constant. Verification that MMC_{red} was present after catalytic reduction of MMC_{ox} was carried out by purging the dimethyl sulfoxide stock solution of the hydroquinone with air followed by evaporation *in vacuo*. The ^1H NMR spectrum of the residue in dimethyl sulfoxide-d_6 was identical to that of authentic MMC_{ox}.

The dimethyl sulfoxide stock of the $\mathbf{1_{red}}$ was prepared by reduction of $\mathbf{1_{ox}}$ in the presence of H_2 and 5% Pd on carbon. The procedure employed was the same as that described for the reduction of MMC_{ox}, except that water was not added to the dimethyl sulfoxide. Oxidation of the $\mathbf{1_{red}}$ stock by addition of air afforded $\mathbf{1_{ox}}$, indicating that decomposition of the reduction product had not occurred. The kinetic studies were carried out by adding 50 μL of $\mathbf{1_{red}}$ stock to 2.95 mL of anaerobic buffer and then collecting absorbance (320 nm) vs time data with a UV–vis spectrophotometer at 30.0 ± 0.2 °C.

The pH rate laws for the reaction studied herein were derived by material balance, see Bruice and Benkovic[31] for details.

Spectrophotometric pK_a Determinations were carried out for pK_{a1} of $MMC_{ox}H_3^{3+}$, for $\mathbf{1_{ox}H^+}$, and for $\mathbf{3_{ox}H^+}$. The pK_a determinations were made by computer-fitting absorbance vs pH data, obtained in μ = 1.0 (KCl) 30.0 ± 0.2 °C aqueous buffer, to the following equation:

$$\text{absorbance} = \frac{A_T a_H \epsilon_{HA} + A_T \epsilon_A K_a}{a_H + K_a} \qquad (10)$$

where A_T is the total concentration of acid and conjugate base ([AH] + [A]), ϵ_{AH} is the extinction coefficient of the acid form, ϵ_A is the extinction coefficient of the conjugate base, a_H is the proton activity determined with a glass electrode, and K_a is the acid dissociation constant obtained from the fit. Rapid decomposition of MMC_{ox} in strong acid required extrapolation of the absorbance values to t = 0. Absorbance vs time data obtained from the hydrolysis study of MMC_{ox} (Figure 1) was extrapolated to t = 0 using the first-order rate law. Neither $\mathbf{1_{ox}}$ nor $\mathbf{3_{ox}}$ exhibited hydrolysis during the absorbance measurements in strong acid.

Electrochemistry. A stock solution of MMC_{ox} or $\mathbf{1_{ox}}$ (0.05 mmol) was prepared in dry dimethyl sulfoxide. Measurements were carried out by adding 100 μL of the stock solution to 4.9 mL of μ = 1.0 ($NaClO_4$) aqueous buffer at 25 to 26 °C under an atmosphere of argon in a BAS C-27A cyclic voltammograph. A BAS Ag/AgCl gel electrode was the reference and a Pt electrode was the auxiliary. A graphite mull was employed as the working electrode.[32] The reference electrode was calibrated against the E_o value of benzoquinone/hydroquinone (699 mV, NHE). The scan speed was 100 mV s^{-1}.

Preparation of 1-Acetoxy-7-amino-6,9-dimethyl-2,3-dihydro-1*H*-pyrrolo[1,2-*a*] indole-5,8-dione ($\mathbf{1_{ox}}$) was carried out from the 1-hydroxy derivative previously reported in the literature:[33] To a solution of 70 mg (0.28 mmol) of the 1-hydroxy derivative in 10 mL of dry pyridine cooled to 5 °C was added 7 mL of freshly distilled acetic anhydride and the mixture was stirred at 10 to 25 °C for 2 h. The reaction mixture was poured into 100 mL ice-cold water and extracted with 2 × 50 mL portions of ethyl acetate. The extracts were washed in water, dried (Na_2SO_4), and concentrated to afford a red gum. The product was purified by flash chromatography over silica gel using chloroform/ethyl acetate (90:10) as the eluant. Recrystallization of the purified solid from chloroform/hexane afforded $\mathbf{1_{ox}}$ as red crystals: 58 mg (71%); mp 172–173 °C; TLC (chloroform/methanol [95:5]) R_f = 0.70; IR (KBr pellet) 3447, 3306, 2924, 1738, 1668, 1591, 1489, 1385, 1356, 1246, 1107, 1022 cm^{-1}; ^1H NMR ($CDCl_3$) δ 6.03 (1H, dd, J = 1.6 Hz, J = 6.6 Hz, 1-methine proton), 4.88 (2H, bs, NH_2), 4.35–4.20 (2H, m, 3-diastereomeric methylene protons), 3.00–2.78 (1H, m, 2-diastereomeric methylene proton), 2.54–2.47 (1H, m, 2-diastereomeric methylene proton), 2.27 (3H, s, acetate methyl), 2.04 and 1.81 (6H, 2s, methyl); mass spectrum m/z 288 (M^+), 229 (M^+ – $OCOCH_3$), 201, 184, 138, 122, 108. Anal. Calcd for $C_{15}H_{16}N_2O_4$: C, 62.49; H, 5.59; N, 9.72. Found: C, 62.57; H, 5.65; N, 9.63.

Hydrolysis Studies of $\mathbf{1_{red}}$. A solution of 10 mg (0.035 mmol) of $\mathbf{1_{ox}}$ in 1.5 mL of dimethyl sulfoxide was added to a suspension of 10 mg of 5% Pd on carbon in 10 mL of buffer (1 M acetate or 0.2 M phosphate, μ = 1.0 KCl) held at pH 5, 6, 7, 7.5, 8, or 9. The reaction mixture was degassed with argon for 10 min and then purged with hydrogen gas until the solution became colorless (~10 min). Finally, the reaction mixture was degassed for 20 min and incubated at 30 °C for 18 h under strict anaerobic conditions. The reaction was opened to air, stirred for 20 min, and then filtered through Celite. The filter cake was washed 2× with 20 mL portions of $CHCl_3$, and the filtrate was extracted 2× with 50 mL portions of $CHCl_3$. The combined chloroform extracts were washed with water, dried (Na_2SO_4), and concentrated to a solid red mass. Preparative thin-layer chromatographic separation over silica gel using $CHCl_3$ as the eluant afforded $\mathbf{4_{ox}}$ and $\mathbf{5_{ox}}$, the physical properties of which are provided below.

7-Amino-2,3-dihydro-1-hydroxy-6,9-dimethyl-1*H*-pyrrolo[1,2-*a*]indole-5,8-dione ($\mathbf{4_{ox}}$) was recrystallized from chloroform to afford deep red crystals: mp 196–198 °C; TLC (chloroform/methanol [90:10]) R_f = 0.40; IR (KBr pellet) 3457, 3422, 3354, 2924, 1667, 1607, 1489, 1393, 1352, 1107, 1072 cm^{-1}; ^1H NMR ($CDCl_3$) δ 5.17 (1H, doublet of triplet, J = 1.9 Hz, J = 6.1 Hz, methine proton), 4.85 (2H, bs, NH_2), 4.35–4.23 (2H, m, 3-diastereomeric methylene protons), 2.82–2.72 (1H, m, 2-diastereomeric methylene proton), 2.49–2.41 (1H, m, 2-diastereomeric methylene proton), 2.32 and 1.80 (6H, 2s, 6,9-dimethyl), 1.74 (1H, d, J = 5.5 Hz, OH); mass spectrum m/z 246 (M^+), 229 (M^+ – OH), 202, 161, 134, 106, 91. Anal. Calcd for $C_{13}H_{19}N_2O_3 \cdot 0.25H_2O$: C, 62.26; H, 5.83; N, 11.17. Found: C, 62.36; H, 5.77; N, 11.02.

7-Amino-2,3-dihydro-6,9-dimethyl-1*H*-pyrrolo[1,2-*a*]indole-5,8-dione ($\mathbf{5_{ox}}$) was recrystallized from hexane as red crystals: mp 208–210 °C; TLC (chloroform/methanol [90:10]) R_f = 0.75; IR (KBr pellet) 3468, 3360, 2987, 2918, 1614, 1574, 1483, 1371, 1342, 1298, 1190, 1098 cm^{-1}; ^1H NMR ($CDCl_3$) δ 4.78 (2H, bs, NH_2), 4.17 (2H, t, J = 7.1 Hz, 3-methylene protons), 2.7 (2H, t, J = 7.2 Hz, 1-methylene protons), 2.52 (2H, quintet, J = 7.2 Hz, 2 methylene protons), 2.20 and 1.80 (6H, 2s, 6,9-dimethyl); mass spectrum (El) m/z 230 (M^+), 203 (M^+ – HCN), 186, 174, 159, 146, 131, 118, 101. Anal. Calcd for $C_{13}H_{14}N_2O_2$: C, 67.80; H, 6.13; N, 12.17. Found: C, 67.87; H, 6.18; N, 12.13.

Acknowledgment. The research was supported by an award from the National Science Foundation.

JO941679Q

(31) Bruice, T. C.; Benkovic, S. J. *Bioorganic Mechanisms*; W. A. Benjamin, Inc.: New York, 1966; Vol. 1, pp 4–16.

(32) Construction of the electrode is described in the following reference: Skibo, E. B.; Bruice, T. C. *J. Am. Chem. Soc.* **1983**, *105*, 3304–3315.

(33) Boruah, R. C.; Skibo, E. B. *J. Med. Chem.* **1994**, *37*, 1625–1631.